Vietnam Academy of Science and Technology

Vietnam Journal of Marine Science and Technology

journal homepage: vjs.ac.vn/index.php/jmst

Research for forecasting the effect of various meteorological-dynamic conditions on the possible spreading of Cs-137 radioactive substances in case a level 7 incident occurs from Fengcheng nuclear power plant (China)

Nguyen Minh Hai[1], Vu Duy Vinh[1,*], Nguyen Trong Ngo[2], Tran Quang Thien[2]

[1]*Institute of Marine Resources and Environment, VAST, Vietnam*
[2]*Dalat Nuclear Research Institute, Lam Dong, Vietnam*

Received: 31 December 2021; Accepted: 30 June 2022

ABSTRACT

Because its location is quite close to the Vietnamese border, the future operation of the Fengcheng (Fengcheng) Nuclear Power Plant (NPP) can raise many concerns about the impact on the marine environment in case a serious incident occurs. Based on the Delft3D modeling toolkit, calculation scenarios to simulate the spreading of Cs-137 radioactive emission when a level 7 incident occurs at Fengcheng NPP have been set up according to different dynamic/meteorological conditions presented at the time of incidents (during the Northeast monsoon, transitional monsoon, or Southwest monsoon) to assess/predict the possibility of radioactive emission and to spread, and their affecting the waters of Vietnam. The simulation results show that when a level 7 incident occurs from Fengcheng NPP, the area of influence might be the entire East Sea after 3–6 months. The Gulf of Tonkin area would be contaminated with high radiation levels (300–350 Bq/m^3) after about one month. The radiation would then gradually decrease to less than 150 Bq/m^3 after one year and below 30 Bq/m^3 after two years. The impacts of various dynamical and meteorological conditions on the ability to spread and disperse radioactive substances when an incident occurs are only evident in the early stages (up to 3 months after the incident). After this time, the contaminated area would cover almost the entire coastal strip of Vietnam due to a large amount of radiation, and the effects of different dynamic/meteorological conditions would be irregular.

Keywords: Delft3D, Fangchenggang, nuclear power plant, Cs-137 radioactive emission.

[*]Corresponding author at: Institute of Marine Resources and Environment, 246 Da Nang, Ngo Quyen, Hai Phong, Vietnam. *E-mail addresses:* vinhvd@imer.vast.vn

https://doi.org/10.15625/1859-3097/15964
ISSN 1859-3097; e-ISSN 2815-5904/

INTRODUCTION

Although the highest safety standards must always be followed, the operation of nuclear power plants (NPPs) is always a cause for serious concern because if something goes wrong, the consequences can be severe, not only for the ecological environment but also for human life and health. Therefore, the assessment and prediction of the possibility of the impact and the mechanism of transmission and distribution of radioactive substances when an incident occurs are critical in providing scientific information on the possibility of the impact if an incident occurs, as well as improving the method of assessment and prediction of radioactive propagation in the sea.

Among the approaches, modeling is a widely used direction in the study and prediction of the areal extent and the impact level caused by radioactive leakage to the marine environment. This method not only overcomes the limitations and difficulties of the traditional method of surveying but also can evaluate and forecast under different scenarios, thereby providing information about the potential propagation, dispersal, areas of influence, and factors affecting this process when radioactive nuclear leakage occurs [1–6]. However, the use of radiological propagation simulation modeling tools is still limited due to the difficulty of input data and data calibrating and verifying the simulation calculation results. Therefore, to improve the accuracy, quite a few studies have been carried out in the direction of retrospectively recalling the nuclear incidents occurred [7].

The Fengcheng Nuclear Power Plant is located in Guangxi, China, just 50 km from Quang Ninh province of Vietnam. As recommended by the International Atomic Energy Agency (IAEA), the area outside a nuclear power plant with a capacity of more than 1,000 MW needs to be zoned for an appropriate incident response plan: an emergency protection zone (emergency planning zone, PAZ) from 3–5 km; emergency protection planning area (possibly populated but must have a response plan to prevent irradiation to the public outside the facility when an incident occurs, UPZ) from 15–30 km; extended planning distances (EPD) at less than 100 km and cargo and food planning distances (ICPD) less than 300km. Thus, Quang Ninh and some northern provinces of Vietnam are also in the EPD and ICPD regions relative to Fengcheng NPP, and Vietnam needs to prepare contingency plans. Although there are many concerns about the effects of a radioactive incident from China's nuclear power plants on our waters, scientific studies on these effects are very few, especially quantitative research on the scope and extent of impact if an incident occurs [8]. This study is conducted based on the hypothesis of an accident from Fengcheng NPP with an incident level of 7, equivalent to the Fukushima accident. A modeling system has been established with different failure scenarios based on the Delft3D model. The research results will provide more insights into the extent and scope of the incident and the impact of meteorological conditions and dynamics on the propagation and distribution of radiation when an incident occurs.

MATERIALS AND METHODS

Materials

The materials used in this study include two groups of documents: serving to set up hydrodynamic models and establish radiological propagation and dispersion models when incidents occur. The documents used to establish hydrodynamic models include depth and shoreline data in the study area. These are UTM topographic maps with geographic coordinates system VN 2000 at scale 1:50,000 and 1:25,000. The depth of the outer area using GEBCO -1/8 database with 0.5 min resolution processed from satellite images combined with depth data [9–10]. The meteorological data used for this study are the spatial wind, barometric, and temperature fields of the entire East Sea region with a resolution of 0.2 degrees of NCEP-National Centers for Environmental Prediction [11] in the intervals of simulation time of the model. These data series will be included in the model as spatial data arrays

with time steps of 6 h/time. Water level data to be used for model calibration every hour at Hon Dau, Bach Long Vi, Hon Ngu, and Con Co in 2018 and 2019. In addition, the tidal harmonic constant database with 13 the main tidal components are *M*2, *S*2, *K*2, *N*2, *O*1, *K*1, *P*1, *Q*1, *MF*, *MM*, *M*4, *MS*4, and *MN*4. These tidal harmonic constants were collected and processed from the LEGOS FES2014 tidal constants database [12] and TPXO8 Atlas of Oregon State University (USA) [13]. The WOA13 database [14], with a resolution of 0.25 degrees for the East Sea area, was also exploited to be used as input for the thermal-salt boundary conditions of the outer model. The average monthly river discharge of rivers along the coast of Vietnam is used as the river boundary conditions of the model. Documents on water level fluctuations measured by the National Hydro-Meteorological Center at coastal stations such as Hon Dau, Bach Long Vi, Hon Ngu, Con Dao, and Vung Tau are also used to verify the water level measurement data of the model. Besides, the flow measurement data in the coastal areas of Vietnam of many topics and projects implemented in recent years have also been used to calibrate and verify the results of the model's flow calculation.

A group of related documents on the physical properties of nuclear radioactivity and simulation results of radioactive material emission assessment when a nuclear accident occurs are also used and referenced for establishing a mathematical model [3, 9, 15].

Methods

Model selection

The propagation, diffusion, and transport of matter in the aquatic environment depend mainly on hydrodynamic processes - directly from the water mass movement. In this study, the main research subjects, such as hydrodynamics (including temperature and salinity) in the East Vietnam Sea, were modeled based on the Delft3D model. In Vietnam, the Delft3D model has also been used to study hydrodynamic processes, e.g., sediment transport and erosion in the coastal areas of Hai Phong, Ha Long, along the banks of the Red River Delta, and some lagoon areas in the central region, and along the banks of the Mekong Delta [4, 5, 16–20]. Delft3D has also been used to simulate water quality processes, contaminant propagation, oil spills that occur in some other sea areas in Vietnam [21–23], and propagation of radioactive emission according to Fengcheng NPP accident scenarios of 5-, 6-, and 7-level that may occur [8].

This study uses the Delft3D-Part (particle tracking) module, using the results from the hydrodynamic model, to simulate radioactive release when a radioactive leak occurs. Pollutant traces are determined in 3 dimensions over time based on the variation of the pollutant distribution content on a grid cell. The primary method of this model is based on random movement from which the movement of matter is simulated statistically with a defined number of particles. The Delft3D-Part model simulates spatial and temporal changes in material concentrations under different dynamic conditions in estuaries, coastal areas, and the sea [24]. The basic physical processes of the model include 1) Emission sources (continuous or instantaneous); 2) Determined material source (concentration, weight, physical and chemical properties); 3) Time variation of wind field and influence of surface wind on transport; 4) The deposition (sinking) and resuspension (bottom erosion) of matter; 5) Decomposition over time. At any location, the matter will be affected by three main processes: transport due to the movement of the water mass (advection), diffusion/dispersion, and deposition (including deposition and resuspension).

Range and mesh of the model

Because the spread and emission of radiation can extend to the entire East Vietnam Sea area, the model's domain range covers the entire area. The grid used for the model is a complex orthogonal curved grid system in the coastal areas and islands and less in the offshore area where the terrain is relatively invariable. The calculated area has a size of about 2,800 km in the North-South direction and 2,550 km in the East-West direction,

divided into 404 × 938 points with grid cells varying in size from 47.5 m to 21,197 m (Figure 1a).

The grid cells are calculated vertically using the coordinate system σ divided into eight layers of water with equal proportions from the surface to the bottom of 12.5% depth for each water layer. The depth grid is established based on the grid and the topographic map of the area.

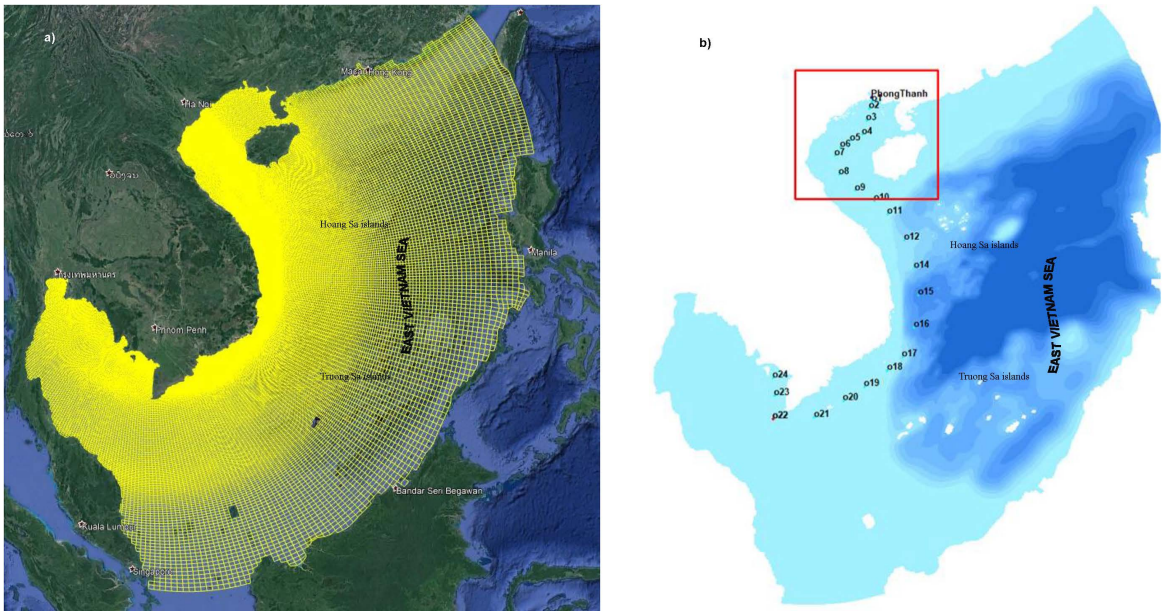

Figure 1. The grid of the model (a) and the locations of the test points (b)

Set calculation time

The synthetic model for the coastal waters of the East Vietnam Sea region was established and run between 2018 and 2019. The calculation time step is 0.5 min.

Basic processes

The computational model is selected for the simultaneous association of the basic hydrodynamic-wave-sediment transport processes [26]. The main factors to be considered include salinity, temperature; the influence of surface winds; interaction with waves (simultaneous wave-online coupling).

Boundary conditions

The model has open sea and river boundaries. The river openings include the entire primary river system of Vietnam, including the Red-Thai Binh river system, the Mekong River, and the rivers in the central region. For river boundaries, the salinity, temperature, and flow data used are the monthly average values calculated from the survey data of the project and measurements from the fixed monitoring stations of the National Hydro-Meteorological Center. Meanwhile, the sea-side thermal–salt boundary condition uses data from the World Ocean Atlas 2013 database (WOA13).

The open seaward boundaries of the model include the Kalimantan Straits (Indonesia), Sulu Strait, Mindanao, Luzon (Philippines), and Bashi Strait (Taiwan). Given the sea boundary conditions, the data to provide these open boundaries are the tidal harmonic constants of the 13 main tidal components, which are *M*2, *S*2, *K*2, *N*2, *O*1, *K*1, *P*1, *Q*1, *MF*, *MM*, *M*4, *MS*4, and *MN*4. These tidal harmonic constants were collected and processed from the LEGOS' FES2014 database [12].

Set the model's initial conditions

In the Delft3D model, the model's initial conditions can be used from the calculation results of previous runs through restart files. For the case applied to the study area, due to the large domain, there is a significant difference in salinity, temperature, and water level, so the initial conditions of the hydrodynamic model are calculated results in the range of 3 months before radioactive emission simulation.

Meteorological conditions

There are coastal hydrometeorological stations in our waters, such as Co To, Hon Dau, Bach Long Vi, Hon Ngu, Vung Tau, and others. However, wind data measured at these stations are usually sparse (6 h/time) and unevenly distributed in space. Therefore, in this study, wind field data, barometric pressure, air temperature, solar radiation, and cloud volume are included in the model as spatial data arrays with a time step of 3 h/time of NCEP (National Centers for Environmental Prediction) [11].

Verify the results of the hydrodynamic model

To evaluate the reliability and effectiveness of the model, in this study, the model reliability index *E* (Nash) [25, 26] was used. This is the index that evaluates the number of forecasts that guarantee the allowable reliability [26]:

$$E = 1 - \frac{\sum_{i=1}^{n}\left(O_i - P_i\right)^2}{\sum_{i=1}^{n}\left(O_i - \bar{O}\right)^2}$$

The value of *E* approaching 1, the forecasting results have the best performance, whereas when *E* approaches 0, the forecasts are unreliable. According to the published results of Moriasi et al. [27], the model is acceptable with the E coefficient in the range of 0.5–0.65 and good if this coefficient is in the range of 0.65–0.75. When E has a negative sign (-), the average features calculated from the observed series give better prediction results from the model [25].

Radioactive dispersion model

The radiation propagation model is established based on the hydrodynamic model results and uses the following groups of results: Domain extent, grid, topography; Calculation results of water level fluctuations, flow fields; Calculation results of temperature, salinity; Bottom stress field. In this study, the radioactivity of choice was Cs-137, a radioactive cesium isotope formed by the nuclear fission of uranium 235 and other fissile isotopes in nuclear reactors. Cs-137 has a specific density of about 1,800–1,900 kg/m^3 and a decomposition period of about 30.05 years.

The dispersion coefficient of the model is used according to the formula of Bent et al. [28]. After being adjusted and selected, the coefficients a and b are 1.5 and 0.7, respectively. The model can also consider the processes of radioactive exchange through the sediment. In this study, we ignore the re-suspension to the aquatic environment of radioactivity from the sediments and account only for the bottom deposition of radioactivity from the water column. The sedimentation coefficient of the material element in the Delft3d -Part model is determined through the correction processes. After correction, the non-periodic velocity component (*A*0) was selected with a value of 0.0005 m/s, while the time variable cyclic velocity component was selected as 0 m/s.

Simulation calculation scenarios

According to the International Atomic Energy Agency (IEAE) classification, nuclear incidents include seven levels [29], of which the highest level is level 7, which is a severe accident. The Fukushima nuclear plant accident was rated at 7. After this incident, various studies were conducted to determine the radiation released from this plant into the sea. However, this is an extremely difficult task, so the claims about this radiation are varying: 14.5 × 1,015 Bq [30]; 16.2±1.6 × 1,015 Bq [31]; 11–16 × 1,015 Bq [32]. These

values are very different from those published by Japanese authors, showing only about 3.5 × 1,015 Bq [5, 33, 34]. This study assumes that the radioactive leakage from Fengcheng NPP is about 3.5 × 1,015 Bq, like related studies [5, 33, 34], and the radioactive leak time is 15 days since the incident occurred. For each scenario group, the event time is assumed during the northeast monsoon (NE), the transition season from northeast wind (NE) to the southwest wind (SW), and southwest wind (SW) and the transition season from southwesterly winds (SW) to northeasterly winds (NE). The calculation and simulation time for each scenario is from the time of the incident and lasts two years. Studies related to the Fukushima NPP incident had shown that the radioactive matter released into the atmosphere only occurred in the first 4–5 days when the NPP accident happened. Then due to radioactive clouds being destroyed and transported very far, the amount of radiation from the air brought down to the sea surface was insignificantly small [4, 5]. Therefore, in this study, we did not consider additional radioactive matter from the air.

RESULTS AND DISCUSSION

Distribution and dispersion of radiation in different incident conditions

The results clearly show a significant difference in the amount of radiation emitted and the radiation spread from near the incident site to the waters of the East Vietnam Sea. However, due to a large amount of radioactive leakage, the influence of meteorological and dynamic conditions is only evident in the first stage (less than three months since the incident occurred). After that, when the amount of radiation was spread to the entire East Vietnam Sea, the scope and influence of the cases differed insignificantly and affected most of the East Vietnam Sea. About one month after the incident, the Gulf of Bac Bo's sea area was contaminated with Cs-137 content up to 300–350 Bq/m^3. The extent of radioactive fallout under the influence of the Northeast monsoon and the transitional monsoon from Southwest to Northeast is more remarkable than when the incident occurred in the southwest monsoon and the Northeast-to-Southwest monsoon season. In particular, when the incident occurred during the southwest monsoon season, due to the direction of impact of wind fields (wind fields S, SW, and SE) opposite to the direction of radiation propagation, the disturbance of Cs-137 radiation increased in the aquatic environment (Figure 2a, d, g, k). The contaminated area then expanded and covered almost the entire East Vietnam Sea area after 3–6 months. Radioactive substances are highly concentrated in the coastal areas of the Gulf of Tonkin, and in the coastal areas of the Mekong river delta, with radioactive Cs-137 concentrations of about 150–250 Bq/m^3 (Figure 2b, e, h, l). The radioactive content of Cs-137 in water decreased slowly to less than 150 Bq/m^3 after one year (Figure 2c, f, i, m). After two years after the incident, the entire coastal strip of Vietnam still has a Cs-137 value below 30 Bq/m^3.

Impact of dynamical and meteorological conditions at the time of the incident on the fluctuation of radioactive volume over time and with depth

The distribution of radioactive substances over time and depth is evaluated by calculating the average radioactive content of each month within two years at some points along the coast of Vietnam (Figure 1b).

Because the amount of radiation released into the environment is quite large when a level 7 incident occurs at the *O*1 point area (near the incident place) (Figure 1b), the simulation results show that the surface radiation has a high value and there is no significant difference between cases. The average amount of radiation can be above 100,000 Bq/m^3 in the first month, then drops below 1,000 Bq/m^3 after two months. From the 3rd to the 24th month, radioactive material decreased slowly between months, ranging from 50–100 Bq/m^3 (Figure 3a).

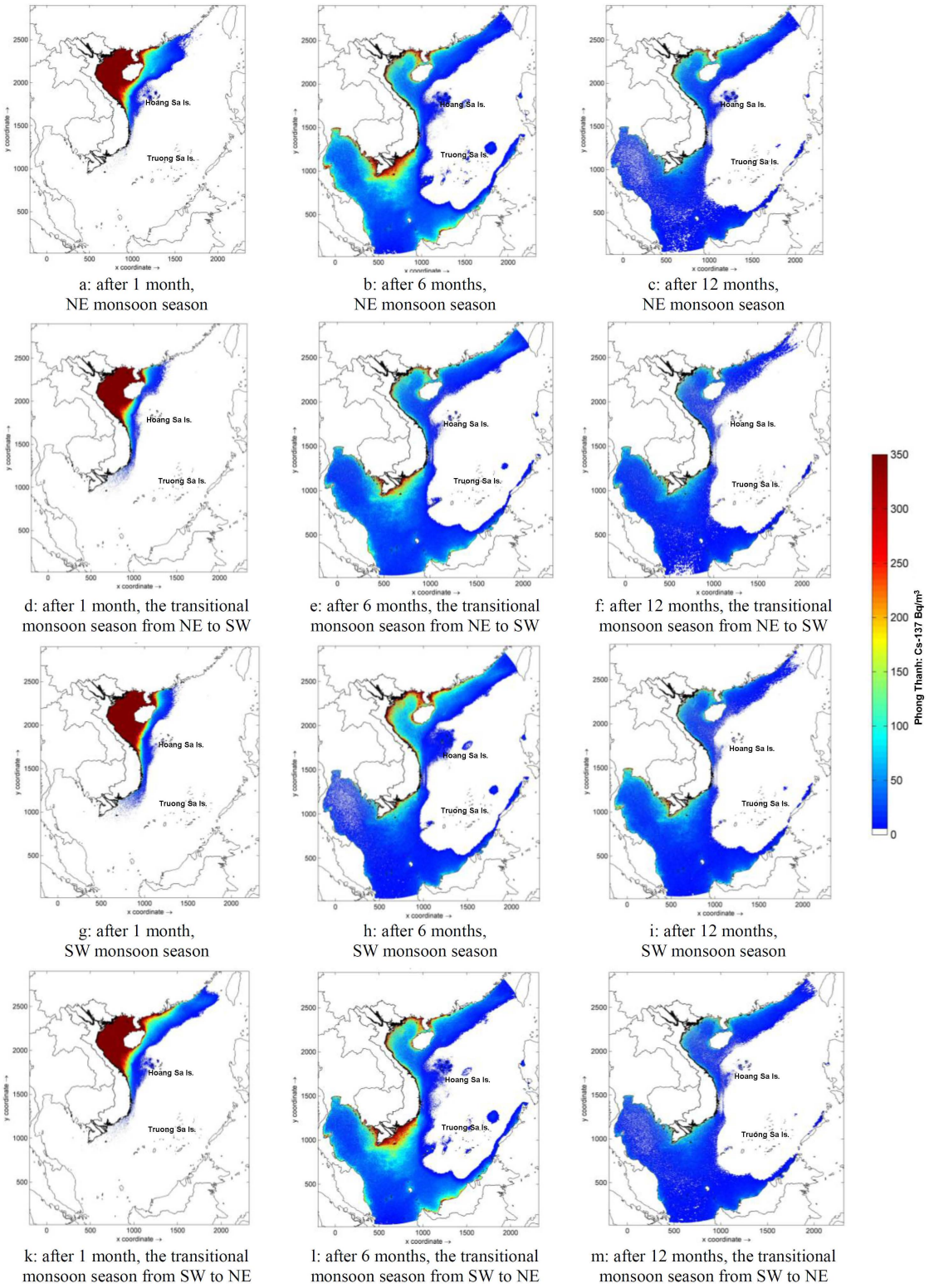

a: after 1 month, NE monsoon season
b: after 6 months, NE monsoon season
c: after 12 months, NE monsoon season
d: after 1 month, the transitional monsoon season from NE to SW
e: after 6 months, the transitional monsoon season from NE to SW
f: after 12 months, the transitional monsoon season from NE to SW
g: after 1 month, SW monsoon season
h: after 6 months, SW monsoon season
i: after 12 months, SW monsoon season
k: after 1 month, the transitional monsoon season from SW to NE
l: after 6 months, the transitional monsoon season from SW to NE
m: after 12 months, the transitional monsoon season from SW to NE

Figure 2. Forecast of Cs-137 concentration distribution (Bq/m^3) in the middle layer when an accident occurs at Fengcheng NPP

In addition, the analysis results of monthly average radioactivity at point *O*1 show an apparent fluctuation of radioactive concentration with depth under different influences of meteorological and dynamical conditions. Radioactivity tends to be markedly higher in the upper aquifers (layers 1 to 3) than in the bottom layers (Figure 3). It is noteworthy that the effects of meteorological-dynamic conditions on the radioactivity content in different aquifers did not show the same trend as in the surface layer, thus, representing the complexity in the propagation and distribution of radiation. The results of simulation calculations show signs of radiation conservation: high concentrations in this aquifer must have lower values in other aquifers and vice versa (Figure 3). Also, at the *O*1 point area, the analysis and evaluation results show that the amount of radiation was only presented at the bottom of this area for about the first six months after the incident. After that, the amount of radioactivity in the bottom layer of the *O*1 point area decreased sharply and dropped to a value below 1 Bq/m^3 (Figure 3d).

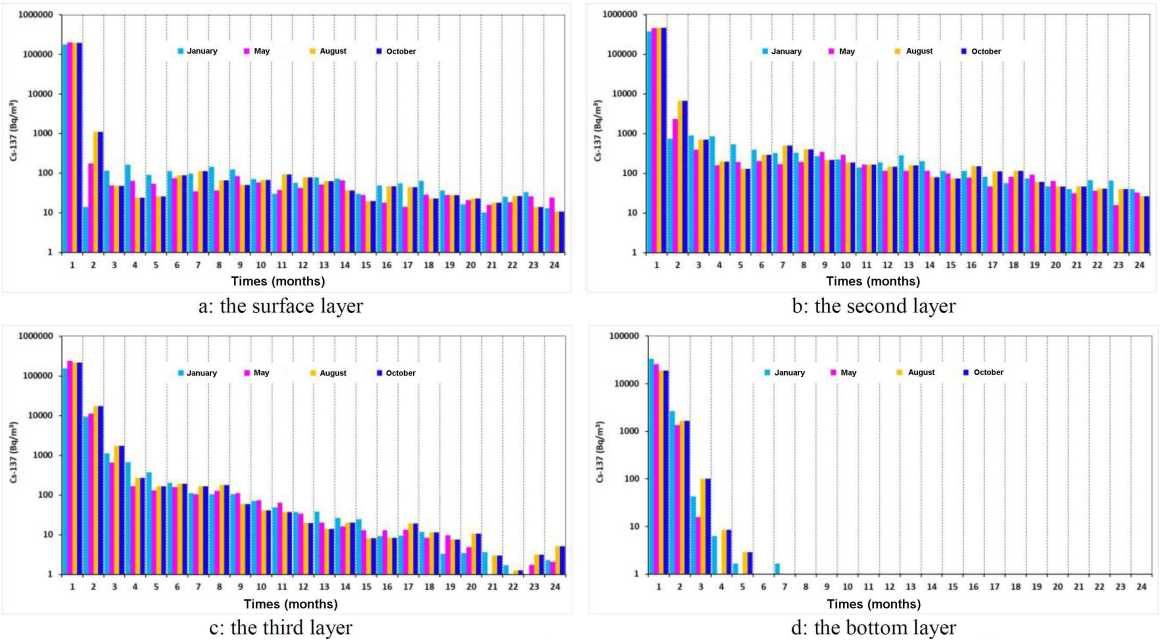

a: the surface layer

b: the second layer

c: the third layer

d: the bottom layer

Figure 3. Concentration of Cs-137 (Bq/m^3) at point *O*1 in different incident times

In the area between the Gulf of Tonkin (point *O*6), the amount of radioactivity in the surface water fluctuates in the range of 5–1,000 Bq/m^3. In which the radioactive content reached a higher value (over 100 Bq/m^3) in the first and second months, then decreased in the following months. About three months after the incident, the average radioactive content in the surface water layer dropped below 100 Bq/m^3. The average amount of radiation after 1–2 months is higher when the incident occurs during the southwest monsoon season or the Southwest to the Northeast monsoon season and lowest when the accident occurs in the Northeast monsoon season. However, from 3 to 6 months, the trend of radioactive change is contrasting, high in case the incident occurs in the Northeast monsoon season. After two years after the incident, the radioactive amount in the surface water still reaches values around 1–5 Bq/m^3, and lower in the case of a nuclear power plant incident occurring in the Southwest monsoon and wind color transitions from Southwest to Northeast (Figure 4a).

According to the depth, if in the surface layer the most considerable amount of radiation (in the first two months) is less than 1,000 Bq/m^3, in the lower water layer (the

second, third, and bottom layers), the radioactive amount is higher than 1,000 Bq/m^3. From the third month onwards, the average amount of radioactivity in the water decreases gradually over time. The difference in radioactivity mainly occurs in the surface layer during the first two months, with radioactive values significantly higher if the incident occurs during the Southwest monsoon season and the transition season from Southwest to Northeast wind compared to the first two months. While in the other strata, there is no significant difference in the amount of radiation between the cases. In the area of point *O*6, the fluctuation with the depth of radiation shows a trend: in the surface layer, it gradually increases from the first month to the maximum in the second month after the incident; then, in the middle layers, there is a phase shift in the amount of radiation between January and February that is not much different; to the bottom layer, there is a sharp increase in the amount of radiation from January to February. In addition, the amount of radiation after two years of the incident in this area decreased below 10 Bq/m^3, especially in the bottom layer less than 1 Bq/m^3 (Figure 4).

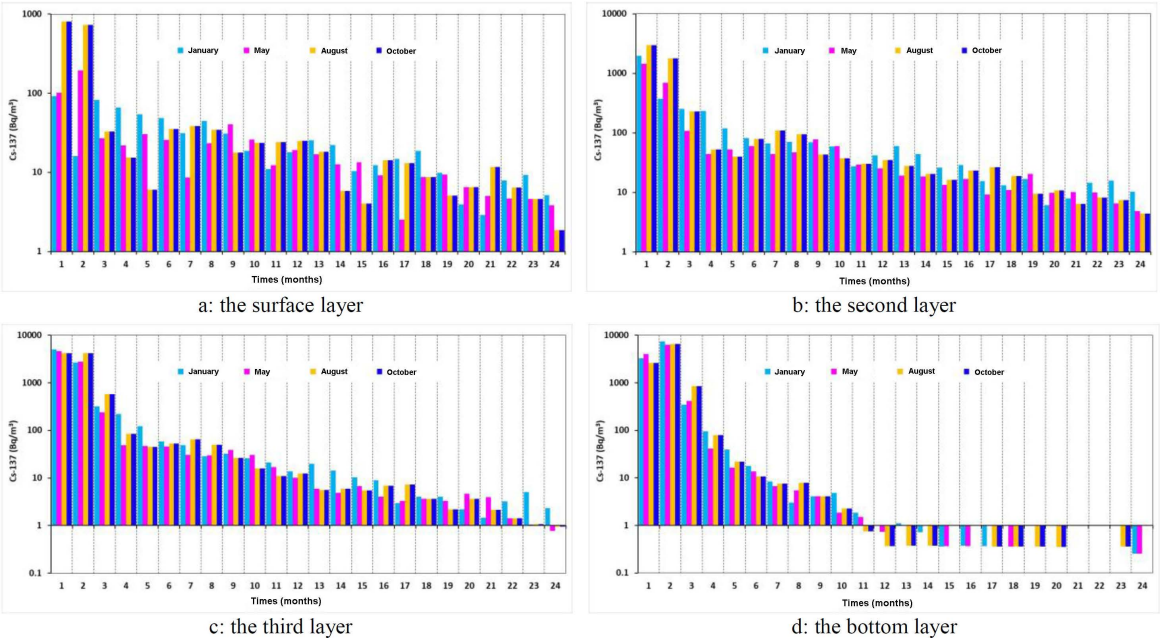

a: the surface layer b: the second layer

c: the third layer d: the bottom layer

Figure 4. Concentration of Cs-137 (Bq/m^3) at point *O*6 in different incident times

In the area around the *O*9 points (near the Gulf of Tonkin mouth), the radioactive amount in the surface water fluctuates in the range of 10–400 Bq/m^3, smaller than in the O6 point area. The fluctuation trend in radioactive concentration increases gradually from January and peaks in the second month (400 Bq/m^3), then decreases sharply in the third month and the following months (below 50 Bq/m^3). When the incident occurred during the southwest monsoon or the transitional monsoon from the southwest to the northeast, the average radiation amount after January and February was higher than in other cases. However, in the next three months, the amount of radiation when it happened in the Northeast monsoon season was higher than in other cases. After two years of the incident, the radiation amount when the incident occurred during the Northeast monsoon season and the transitional monsoon season from Northeast to Southwest still reached 3–5 Bq/m^3, while the remaining two wind seasons are all less than 1 Bq/m^3 (Figure 5a).

For this area, if in the surface layer, the amount of radiation greater than 100 Bq/m^3

only exists in the first two months, then in the lower water layer, such valuable radiation may appear 3–4 months after the incident. The difference in radioactivity mainly occurs in the surface layer and the second layer, with a higher value of radioactive content if the incident occurs during the Southwest monsoon season and the transition season from the Southwest wind to the Northeast wind. While in the two lower floors, the amount of radiation in different incident conditions did not have a big difference. In addition, the variation of radioactivity by strata in this area has changed compared to points in the North: the amount of radiation in all layers has the same tendency to increase gradually from January to reach the highest value after two months and gradually decrease in the following months. After two years of the incident on the 3rd and 4th floors, the amount of radiation fell below 1 Bq/m^3. While in the surface and second layers, the radioactive amount reached 5–10 Bq/m^3 (Figure 5).

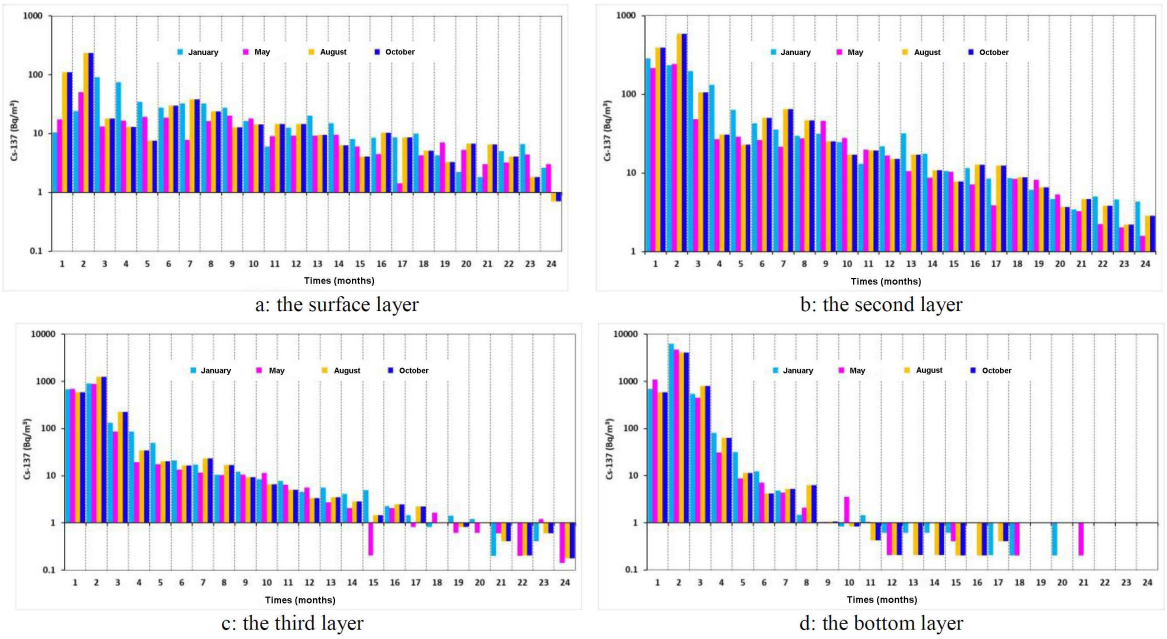

a: the surface layer

b: the second layer

c: the third layer

d: the bottom layer

Figure 5. Concentration of Cs-137 (Bq/m^3) at point *O*9 in different incident times

In the coastal area of Central Vietnam (*O*16), which has the most profound depth on the coast of the East Vietnam Sea, the amount of radioactivity in the surface water decreased sharply, and the typical value fluctuated in the range of 0.1–7 Bq/m^3 significantly more than in the Northern regions. Radioactive concentrations reaching values greater than 1 Bq/m^3 only appear from the 2nd to 12th month after the incident, especially in the 2nd–5th month; it can reach approximately 10 Bq/m^3. From about the 13th month onwards, the average radioactive content in the surface water in this area decreased below 1 Bq/m^3. After two years after the time of the incident, the amount of radioactivity in the surface water in this area still fluctuates around 0.1–0.5 Bq/m^3 (Figure 6a).

The average radioactivity distribution in aquifers also shows a slight upward trend from the surface layer to the third layer and then decreases at the bottom layer. The amount of radiation in the first month is less than 1 Bq/m^3, then more than 5 Bq/m^3 occurs from the second to the 8th month after the incident, especially on the third layer, which can last up to the 12th–13th month. The difference in radioactivity mainly occurs in the surface layer and the second layer, while the remaining two layers do not have a big difference between different cases. Radioactivity was high mainly in the

second to fifth month (5–10 Bq/m^3) and gradually decreased. After two years of the incident, the radiation in this area dropped sharply to below 1 Bq/m^3, except when the incident occurred in the southwest wind color and the transitional monsoon season from Southwest to Northeast on the 3rd floor (greater than 1 Bq/m^3) (Figure 6).

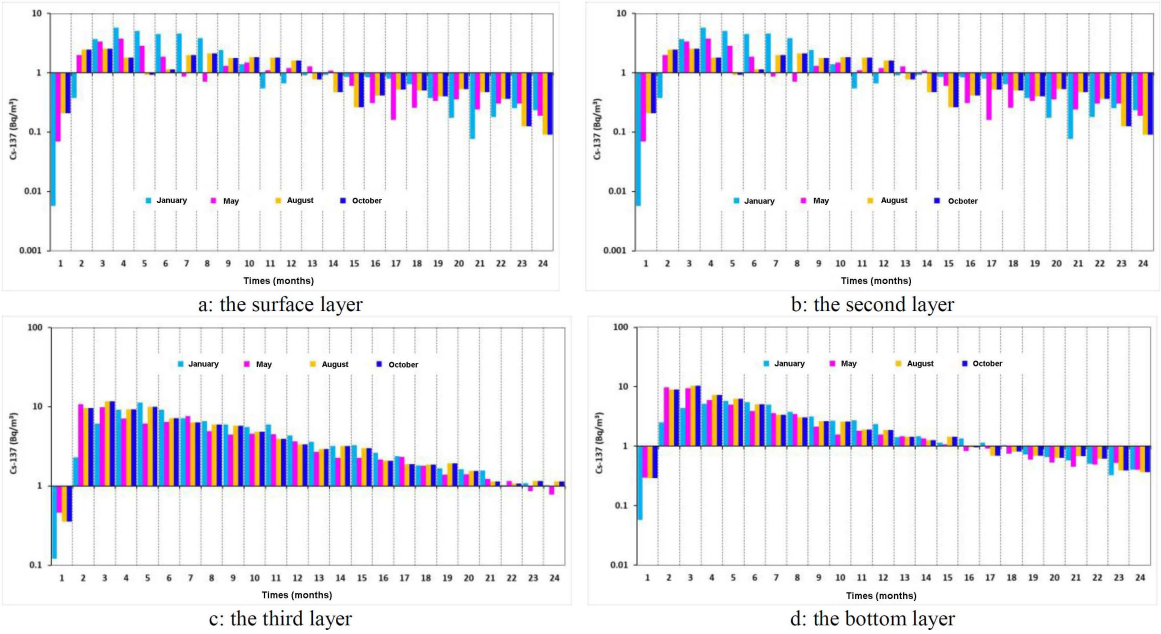

Figure 6. Concentration of Cs-137 (Bq/m^3) at point *O*16 in different incident times

According to the depth, if in the surface layer the amount of radioactivity greater than 50 Bq/m^3 exists from the 4th to the 17th month in some cases, in the second layer of water, such valuable radiation appears again from the 3rd to the 23rd month. Meanwhile, in the third layer, the radioactive content greater than 50 Bq/m^3 only appears from the 4th to the 19th month, and in the water layer near the bottom, most radioactive amounts are less than 10 Bq/m^3 at the beginning of the incident and fall below 1 Bq/m^3 after 24 months. In this area, the amount of radioactivity has a relatively high value in the water layers from the surface to the third layer, with a value of 8–100 Bq/m^3. In addition, the amount of radioactivity in the water in this area after the first month occurs is relatively small, which shows that the effect of radiation from the accident of the nuclear power plant on this area will be evident from the second month on the upper layer and the third month on the lower layer after the incident occurred. Besides, the variation of radioactivity by strata in this area also shows the trend: the highest radioactivity in the surface layer occurs from the second and third month after the incident, then gradually decreases over time. Meanwhile, in the lower aquifer (levels 2, 3, and near the bottom), the average amount of radioactivity increased sharply from January to the second month to the fifth month, reached the highest value after 4–6 months, and decreased gradually in the following months (Figure 7).

In the southern coastal area of the Mekong river delta (point *O*21), radioactive amounts commonly fluctuated between 50–100 Bq/m^3. The calculated and simulated results show that the radioactive content reaching a higher value (above 50 Bq/m^3) appears in the 3rd to 14th month after the incident and decreases gradually in the following months (less than 50 Bq/m^3). The average amount of radiation is high in different cases depending on the time. In the first stage (third to the fifth month) and the last stage (22nd to the 24th month), when the

incident occurs during the transitional monsoon season from Northeast to Southwest, it will be the largest. In the period from the fifth to the 8th month and from the 15th to the 18th month, if the incident occurs in the Northeast monsoon season, the average amount of radiation will be higher than in other cases. For the remaining months, the highest amount of radiation when the incident occurred during the Southwest monsoon season and the transition season from Southwest to Northeast. After two years from the incident, the amount of radioactivity in the surface water in this area still fluctuated around 1–5 Bq/m^3 (Figure 7a).

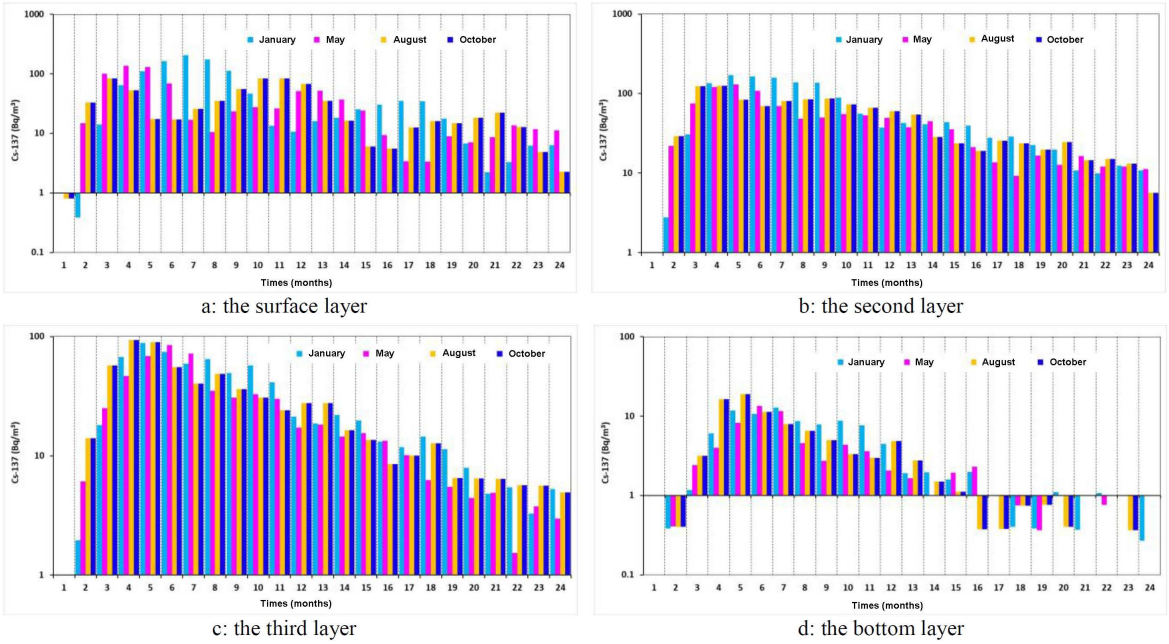

a: the surface layer

b: the second layer

c: the third layer

d: the bottom layer

Figure 7. Cs-137 content (Bq/m^3) at point *O*21 in different incident times

Discussion

According to simulation research results, when an incident occurs, nuclear radiation in the early stages usually exists mainly in the surface water layer as a "cloud" in the water column. During the movement of this contaminated water, radioactive material will continue to move horizontally on the one hand and, on the other hand, will gradually settle down. This observation is consistent with the studies [35–38]. After entering the water environment, radioactive substances will exist in three phases: diffusion, soluble in water; clinging to the particles of suspended matter then deposited to the bottom; penetration into the sediment. However, in this study, the radioactive absorption into the sediment and resuspended from the bottom sediment was not calculated. The general trend is that the first time after the incident, the radiation amount in the surface layer is higher than the lower layers, but over time, the radiation in the upper layers gradually decreases and increases at the bottom.

In this study, the surface layer's most significant amount of radiation appeared in the first month of the incident and gradually slowed down to the South of the East Vietnam Sea. In the Northern areas of the Gulf of Tonkin and the northern part of the East Vietnam Sea, the highest value of surface radioactivity usually occurs in the first month after the incident, while in the central and Southern seas, the largest amount of radiation may appear in the second and the third month in the South-Central coast, and the fourth and fifth month in the Southwestern coastal area. In the vertical direction, the time of occurrence of the maximum radioactive concentration also changes with the decreasing trend of the

difference between the largest amount of radiation appearing in the first month and the following months from the surface layer to the following months in the layers below. Under some conditions, radiation peaks in the lower aquifer can occur 1–2 months later than in the upper aquifers. In addition, the difference in radioactivity over time in the lower aquifers tends to be significantly smaller than in the upper aquifers.

The effects of meteorological and dynamic conditions on the distribution and dispersion of radiation are shown through the difference in monthly average radioactive concentration in each area. Accordingly, when the incident occurs in the Northeast monsoon, the extent of surface radioactive fallout to the southern seas is usually broader. However, the simulation results also show that the effects of the meteorological and dynamic fields are very complex. For example, on the same surface, if an accident occurs in the Northeast monsoon season, it can significantly increase the monthly average radioactive content compared to the case of an incident occurring at other times in the first few months after the accident. However, in the following months, this influence role may be replaced; the radioactive content following an incident occurring during the Northeast monsoon season in those months may become the smallest. Besides, in many areas, if the incident in the Northeast monsoon season increases the radioactive content in the surface layer, on the contrary, in the lower water layer, the radioactive content is due to the influence of the meteorological-dynamic field in the Northeast monsoon season is much smaller than in other cases. Alternatively, there is also a case when an incident in the Northeast monsoon season sharply increased the radioactive content in the first months after the incident occurred; in the last months of nearly two years after the incident, the radioactive content would have the lowest value in case the accident occurred in the Northeast monsoon season. When a level 7 incident occurs, the entire East Vietnam Sea area is contaminated with radiation, especially the Gulf of Tonkin and coastal areas of Vietnam; the radiation can reach over 300 Bq/m^3. The allowable limits of total radioactivity α and β are 0.1 and 1 Bq/m^3, respectively (QCVN 10:2008/BTNMT), which shows that if a level 7 incident occurs, the entire Gulf of Tonkin area will be affected. Vietnam's coastal areas are far beyond acceptable radiation standards and will have a massive impact on the regional resources and environment. Although the amount of radiation has decreased over time, it remains in the water for a long time because this is a relatively closed area with only external water exchange through some straits. After two years, the amount of radioactive substances in the coastal areas of Vietnam still exceeds the allowable standard (over 1 Bq/m^3). The effects of radioactive substances in a level 7 accident are much more severe than when a level 5 or level 6 incident occurs [8].

The analytical evaluation results in this study also show the complexity of the process of radioactive dispersion under the influence of different meteorological and dynamic conditions. Sometimes subject to synergetic effects, but in many cases show the different effects of several factors. The effects of meteorological and dynamic conditions on the distribution and dispersion of radioactive matter are shown through the difference in monthly average radioactive content in each area. Depending on the different stages and areas, the influence role will be replaced, and there is no clear rule. Therefore, within the framework of this report, the laws on the different effects of meteorological and dynamic conditions on the possibility of radioactive dispersion and spread from the Fengcheng NPP's incident to the Gulf of Tonkin and the East Vietnam Sea areas are only preliminary studies. Therefore, it is necessary to have more in-depth studies to confirm the different effects on the distribution and dispersion of radiation or the rules of radioactive propagation if an incident occurs.

CONCLUSION

In order to evaluate and forecast the extent and impact of radioactive sources leaked into

the waters of Vietnam at the highest level following a Fengcheng Nuclear Power Plant accident, a 3-D hydrodynamic-radiation propagation model system has been established with several different scenarios. Predictive simulation results show a specific agreement with related studies.

When a level 7 incident occurs from Fengcheng Nuclear Power Plant, the affected area may be the entire East Vietnam Sea, especially the Gulf of Tonkin, contaminated with high radiation levels (300–350 Bq/m^3). The effects of meteorological and dynamical conditions on the ability to spread and disperse radioactive substances when an incident occurs are only evident in the first three months after the incident. When the contaminated area covers almost the entire coastal strip of Vietnam, the effects of different dynamic/meteorological conditions are no longer evident. The radioactive material was concentrated mainly near the incident site and gradually decreased to the south, but the levels varied depending on the meteorological/dynamic conditions at the time of the incident. According to the depth, the amount of radioactive Cs-137 tends to move gradually between the layers from the surface to the bottom: at first, it is higher in the upper layers, then gradually decreases and increases in the lower layers. The effects of different meteorological and dynamic conditions on the distribution of radioactive substances by depth are also shown but not categorized.

Acknowledgments: The article was supported by the project "Assessment of the current status of the radioactive background of the marine environment in Vietnam, research on the possibility of radioactive dispersion and effects from power plants" and the Task of Protocol "Research, development, and application of a 3D modeling toolkit integrating hydro-thermal dynamic-water quality for monitoring and management of environmental hazards under human impact and climate change". The authors sincerely appreciate such valuable support.

REFERENCES

[1] Honda, M. C., Aono, T., Aoyama, M., Hamajima, Y., Kawakami, H., Kitamura, M., Masumoto, Y., Miyazawa, Y., Takigawa, M., and Saino, T., 2012. Dispersion of artificial caesium-134 and-137 in the western North Pacific one month after the Fukushima accident. *Geochemical Journal*, *46*(1), e1–e9. https://doi.org/10.2343/geochemj.1.0152

[2] Behrens, E., Schwarzkopf, F. U., Lübbecke, J. F., and Böning, C. W., 2012. Model simulations on the long-term dispersal of ^{137}Cs released into the Pacific Ocean off Fukushima. *Environmental Research Letters*, *7*(3), 034004. doi: 10.1088/1748-9326/7/3/034004

[3] Dietze, H., and Kriest, I., 2012. ^{137}Cs off Fukushima Dai-ichi, Japan–model based estimates of dilution and fate. *Ocean Science*, *8*(3), 319–332. https://doi.org/10.5194/os-8-319-2012

[4] Kawamura, H., Kobayashi, T., Furuno, A., In, T., Ishikawa, Y., Nakayama, T., Shima, S., and Awaji, T., 2011. Preliminary numerical experiments on oceanic dispersion of ^{131}I and ^{137}Cs discharged into the ocean because of the Fukushima Daiichi nuclear power plant disaster. *Journal of Nuclear Science and Technology*, *48*(11), 1349–1356. https://doi.org/10.1080/18811248.2011.9711826

[5] Tsumune, D., Tsubono, T., Aoyama, M., and Hirose, K., 2012. Distribution of oceanic ^{137}Cs from the Fukushima Dai-ichi Nuclear Power Plant simulated numerically by a regional ocean model. *Journal of environmental radioactivity*, *111*, 100–108. https://doi.org/10.1016/j.jenvrad.2011.10.007

[6] Estournel, C., Bosc, E., Bocquet, M., Ulses, C., Marsaleix, P., Winiarek, V., Osvath, I., Nguyen, C., Duhaut, T., Lyard, F., Michaud, H., and Auclair, F., 2012. Assessment of the amount of cesium-137 released into the Pacific Ocean after the Fukushima accident and analysis of its dispersion in Japanese coastal waters.

Journal of Geophysical Research: Oceans, *117*(C11). doi: 10.1029/2012JC007933

[7] Buesseler, K. O., Jayne, S. R., Fisher, N. S., Rypina, I. I., Baumann, H., Baumann, Z., Breier, C. F., Douglass, E. M., George, J., Macdonald, A. M., Miyamoto, H., Nishikawa, J., Pike, S. M., and Yoshida, S., 2012. Fukushima-derived radionuclides in the ocean and biota off Japan. *Proceedings of the National Academy of Sciences*, *109*(16), 5984–5988. doi: 10.1073/pnas.1120794109

[8] Vinh, V. D., Hai, N. M., Ngo, N. T., and Thien, T. Q., 2020. Modelling the dispersion of radioactive Cs-137 on the Vietnamese seas due to the Fangchenggang (China) nuclear power plant accident. *Vietnam Journal of Marine Science and Technology*, *20*(4B), 147–162. https://doi.org/10.15625/1859-3097/15919. (in Vietnamese).

[9] Becker, J. J., Sandwell, D. T., Smith, W. H. F., Braud, J., Binder, B., Depner, J., Fabre, D., Factor, J., Ingalls, S., Kim, S-H., Ladner, R., Marks, K., Nelson, S., Pharaoh, A., Trimmer, R., Von Rosenberg, J., Wallace, G., and Weatherall, P., 2009. Global bathymetry and elevation data at 30 arc seconds resolution: SRTM30_PLUS. *Marine Geodesy*, *32*(4), 355–371. https://doi.org/10.1080/01490410903297766

[10] Weatherall, P., Marks, K. M., Jakobsson, M., Schmitt, T., Tani, S., Arndt, J. E., Rovere, M., Chayes, D., Ferrini, V., and Wigley, R., 2015. A new digital bathymetric model of the world's oceans. *Earth and space Science*, *2*(8), 331–345. https://doi.org/10.1002/2015EA000107

[11] Saha, S., Moorthi, S., Wu, X., Wang, J., Nadiga, S., Tripp, P., Behringer, D., Hou, Y-T., Chuang, H-Y., Iredell, M., Ek, M., Meng, J., Yang, R., Mendez, M. P., van den Dool, H., Zhang, Q., Wang, W., Chen, M., and Becker, E., 2014. The NCEP climate forecast system version 2. *Journal of climate*, *27*(6), 2185–2208. doi: 10.1175/JCLI-D-12-00823.1

[12] Carrère, L., Lyard, F., Cancet, M., Guillot, A., and Picot, N., 2016. FES 2014, a new tidal model—Validation results and perspectives for improvements. In *Proceedings of the ESA living planet symposium* (pp. 9–13).

[13] Egbert, G. D., and Erofeeva, S. Y., 2002. Efficient inverse modeling of barotropic ocean tides. *Journal of Atmospheric and Oceanic technology*, *19*(2), 183–204. https://doi.org/10.1175/1520-0426(2002)019<0183:EIMOBO>2.0.CO;2

[14] World Ocean Atlas, 2013. Version 2 (WOA13 V2). Available online: https://www.nodc.noaa.gov/OC5/woa13/

[15] Vinh, V. D., Hai, N. M., and Thao, N. V., 2019. A 3D modeling of the hydrodynamics and waves condition in the North Central coastal area. *Vietnam Journal of Marine Science and Technology*, *19*(3A), 19–31. doi: 10.15625/1859-3097/19/3A/14290. (in Vietnamese).

[16] Vinh, V. D., and Van Uu, D., 2013. The influence of wind and oceanographic factors on characteristics of suspended sediment transport in Bach Dang estuary. *Vietnam Journal of Marine Science and Technology*, *13*(3), 216–226. (in Vietnamese).

[17] Vinh, V. D., Lan, T. D., Tu, T. A., and Anh, N. T. K., 2014. Simulation of characteristic of morphological change in the Me Kong estuary-coastal area. *Vietnam Journal of Marine Science and Technology*, *14*(3A), 31–42. (in Vietnamese).

[18] Vinh, V. D., and Ouillon, S., 2014. Effects of Coriolis force on current and suspended sediment transport in the coastal zone of Red river delta. *Vietnam Journal of Marine Science and Technology*, *14*(3), 219–228. (in Vietnamese).

[19] Vinh, V. D., 2017. Impact of coastal engineering solutions on water exchange and sediment transport in Nai lagoon (Ninh Thuan). *Vietnam Journal of Marine Science and Technology*, *17*(4), 373–385. (in Vietnamese).

[20] Vinh, V. D., and Lan, T. D., 2018. Influences of the wave conditions on the characteristics of sediments transport and morphological change in the Hai Phong coastal area. *Vietnam Journal of Marine*

Science and Technology, *18*(1), 10–26. (in Vietnamese).

[21] Vinh, V. D., 2013. Possible impact in case of oil spill accident in Cua Luc bay. *Petrovietnam Journal*, 04/2013, 56–65. (in Vietnamese).

[22] Vinh, V. D., 2012. Simulation of oil spill in case of oil spill accident in Hai Phong coastal zone. *PetroVietnam Journal*, 03/2012, 48–56. (in Vietnamese).

[23] Vu, D. V., Nguyen, M. H., and Do, G. K., 2020. Impacts of pollution discharges from Dinh Vu industrial zone on water quality in the Hai Phong coastal area. *Vietnam Journal of Marine Science and Technology*, *20*(2), 173–187. (in Vietnamese).

[24] Delft Hydraulics, 2016. Delft3D-FLOW User Manual; Delft 3D-WAVE User Manual, Delft 3D-PART User Manual.

[25] Krause, P., Boyle, D. P., and Bäse, F., 2005. Comparison of different efficiency criteria for hydrological model assessment. *Advances in geosciences*, *5*, 89–97. https://doi.org/10.5194/adgeo-5-89-2005

[26] Nash, J. E., 1970. River flow forecasting through conceptual models, Part IA discussion of principles. *J. of Hyd.*, *10*, 283–290.

[27] Moriasi, D. N., Arnold, J. G., Van Liew, M. W., Bingner, R. L., Harmel, R. D., and Veith, T. L., 2007. Model evaluation guidelines for systematic quantification of accuracy in watershed simulations. *Transactions of the ASABE*, *50*(3), 885–900. doi: 10.13031/2013.23153

[28] Bent, E. J., Postma, L., Roelfzema, A., and Stive, R. J. H., 1991. Hydrodynamic and dispersion modelling of Swansea Bay, UK. *Industrialised Embayments and Their Environmental Problems: A Case Study of Swansea Bay*.

[29] Wheatley, S., Sovacool, B., and Sornette, D., 2017. Of disasters and dragon kings: a statistical analysis of nuclear power incidents and accidents. *Risk analysis*, *37*(1), 99–115. https://doi.org/10.1111/risa.12587

[30] Lai, Z., Chen, C., Beardsley, R., Lin, H., Ji, R., Sasaki, J., and Lin, J., 2013. Initial spread of 137 Cs from the Fukushima Dai-ichi Nuclear Power Plant over the Japan continental shelf: A study using a high-resolution, global-coastal nested ocean model. *Biogeosciences*, *10*(8), 5439–5449. https://doi.org/10.5194/bg-10-5439-2013

[31] Rypina, I. I., Jayne, S. R., Yoshida, S., Macdonald, A. M., Douglass, E., and Buesseler, K., 2013. Short-term dispersal of Fukushima-derived radionuclides off Japan: modeling efforts and model-data intercomparison. *Biogeosciences*, *10*(7), 4973–4990. https://doi.org/10.5194/bg-10-4973-2013

[32] Charette, M. A., Breier, C. F., Henderson, P. B., Pike, S. M., Rypina, I. I., Jayne, S. R., and Buesseler, K. O., 2013. Radium-based estimates of cesium isotope transport and total direct ocean discharges from the Fukushima Nuclear Power Plant accident. *Biogeosciences*, *10*(3), 2159–2167. https://doi.org/10.5194/bg-10-2159-2013

[33] Periáñez, R., Brovchenko, I., Duffa, C., Jung, K. T., Kobayashi, T., Lamego, F., Maderich, V., Min, B-I., Nies, H., Osvath, I., Psaltaki, M., and Suh, K. S., 2015. A new comparison of marine dispersion model performances for Fukushima Dai-ichi releases in the frame of IAEA MODARIA program. *Journal of Environmental Radioactivity*, *150*, 247–269. https://doi.org/10.1016/j.jenvrad.2015.09.003

[34] Kobayashi, T., Nagai, H., Chino, M., and Kawamura, H., 2013. Source term estimation of atmospheric release due to the Fukushima Dai-ichi Nuclear Power Plant accident by atmospheric and oceanic dispersion simulations: Fukushima NPP Accident Related. *Journal of Nuclear Science and Technology*, *50*(3), 255–264. https://doi.org/10.1080/00223131.2013.772449

[35] Margvelashvili, N., Maderich, V., Yuschenko, S., and Zheleznyak, M., 2002. 3-D numerical modelling of mud and radionuclide transport in the Chernobyl

Cooling Pond and Dnieper-Boog Estuary. In *Proceedings in Marine Science* (Vol. 5, pp. 595–609). *Elsevier*. https://doi.org/10.1016/S1568-2692(02)80042-0

[36] Onishi, Y., Kurikami, H., and Yokuda, S. T., 2014. Preliminary Three-Dimensional Simulation of Sediment and Cesium Transport in the Ogi Dam Reservoir using FLESCOT–Task 6, Subtask 2 (No. PNNL-23257). *Pacific Northwest National Lab.(PNNL), Richland, WA (United States)*.

[37] Perianez, R., Abril, J. M., and Garcia-Leon, M., 1996. Modelling the dispersion of non-conservative radionuclides in tidal waters—Part 1: Conceptual and mathematical model. *Journal of Environmental Radioactivity*, *31*(2), 127–141. https://doi.org/10.1016/0265-931X(95)00050-K

[38] Periáñez, R., 2005. Modelling the dispersion of radionuclides in the marine environment. *Springer-Verlag Berlin Heidelberg*.